BIAXIAL TRANSVERSE COMPRESSION TESTING FOR A FIBRE REINFORCED POLYMER MATERIAL

T. Bru[1,2], L.E. Asp[2], R. Olsson[1], G.M. Vyas[1]

[1]Swerea SICOMP, Mölndal, Sweden
Email: thomas.bru@swerea.se, Web Page: https://www.swerea.se/sicomp
[2] Chalmers University of Technology, Department of Industrial and Materials Science, Gothenburg, Sweden

Keywords: Polymer matrix composites, biaxial testing

Abstract
Unidirectional laminates have been tested under uniaxial transverse compression and under biaxial transverse compression. Failure occurred by shear in an inclined failure plane parallel to the fibres. The transverse shear response of the material on the failure plane was evaluated from the tests. In the biaxial tests, the failure load was considerably higher than in the uniaxial tests. For a given transverse shear strain the transverse shear stress was also higher in the case of biaxial compression. It is also shown that using waisted specimens instead of prismatic specimens does not seem to bring noticeable benefits for through-thickness uniaxial compression tests. The experimental results presented here are important input to the development and the validation of damage models of fibre reinforced polymer materials accounting for the matrix nonlinear response in shear and compression.

1. Introduction

In general, during service composite structures develop multiaxial stress states which inevitably affect their mechanical response and their failure. Although the need to better understand the behaviour of fibre reinforced polymer materials under multiaxial stresses was highlighted in the Second World-Wide Failure Exercise (WWFE-II) [1] there are still few existing experimental methods to be used for this purpose. Today biaxial and triaxial testing still relies on relatively large and expensive lab equipment [2, 3].

In this paper, a simple biaxial test method is used to evaluate the behaviour of unidirectional (UD) material under compressive loading normal to the fibre direction. The test setup is inspired from the channel-die setup for plane strain compression of metals, which has also been applied to composites by Collings [4]. It is well accepted that the failure of a UD laminate under transverse compressive stresses is driven by shear. Therefore, the post processing of the test data also consists of extracting the transverse shear response from the compressive stress state. For that, a full field strain measurement technique and stress transformation equations are used. Considering the difficulty in producing high strains in a UD specimen loaded in pure 2–3 shear, the possibility to measure the shear response from a compression test is attractive.

Additionally, uniaxial transverse compression tests are performed using the same specimen geometry as for the biaxial tests. Stress–strain curves and strengths are compared between the two loading types. Finally, the transverse shear stress–strain curves obtained experimentally are compared to the prediction of a constitutive material model accounting for matrix damage.

2. Test setup and specimen information

The specimens were milled from a 36.5 mm thick $[0]_{187}$ laminate which was manufactured by a vacuum infusion process. The reinforcement is a uni-weave non-crimp fabric (NCF) with 12 K carbon fibre bundles in the warp direction and glass/polyamide yarns spaced every 10 mm in the weft direction. The resin is LY556 epoxy and the fibre volume fraction of the laminate is 55%. The material has been extensively characterised in previous in-house tests [5]. The specimens are rectangular prisms of 12x12 mm in the 2–3 plane and 6 to 7 mm in the fibre direction.

The first tests consisted of uniaxial compression of the prismatic specimens in the thickness direction (3–direction). These tests were performed on a 50 kN Shimadzu testing machine using two parallel steel plates with a constant crosshead displacement rate of 1 mm/min. Teflon films (or grease in one case) were used between the steel plates and the specimen to reduce friction. The strains in the 2–3 plane were measured at the specimen surface using the digital image correlation method (DIC) and synchronized with the load. A black and white stochastic pattern was applied to the specimen surface for the DIC measurement. The DIC camera was equipped with a 50/2.8 lens and a 10 mm extension tube. The strain resolution was 0.045% and the spatial resolution 0.09 mm.

A second series of specimens were tested under through-thickness compression while constrained in the 2–direction, therefore producing a σ_{22}–σ_{33} biaxial compressive stress state. The test setup for this loading condition is shown in Fig. 1. The original channel-die concept was kept [4], however pads were introduced between the steel channel and the specimen in order to tailor the ratio of biaxial stresses in the specimen. In this work, the pads were made of plain weave glass/polyester laminates and were oriented so that the through-thickness direction of the pad laminate coincides with the 2–direction of the carbon/epoxy specimen. The pad stiffness in the through-thickness direction was measured to E_{pad}=11.4 GPa. A linear finite element (FE) analysis of the test setup indicated that the stress ratio σ_{22}:σ_{33} was expected to be 1:5.3. The same instrumentation as for the uniaxial compression of unconstrained specimens was used here. In particular, Teflon films were placed between all surfaces to avoid the presence of shear stresses.

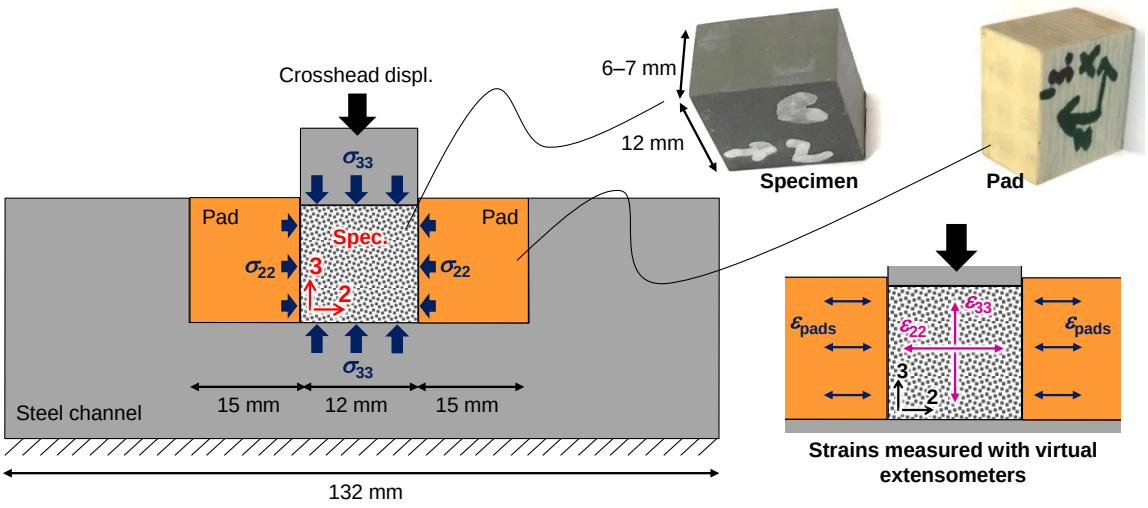

Figure 1. Test setup for the biaxial transverse compression test.

The strains ε_{33} and ε_{22} in the specimen were measured by DIC using virtual extensometers of 9 mm length (an average of three extensometers were used in each case). The stress σ_{33} was evaluated directly from the load measurement and the specimen cross-section. The stress σ_{22} was estimated from

the horizontal strain in the pads, $\sigma_{22}=E_{pad}\cdot\varepsilon_{pad}$, assuming a linear elastic and uniaxial loading of the pads. After each test the stiffness of the pads was measured in a compression test to investigate the risk of damage. No statistically significant variation in stiffness was noticed between the tests.

In total, nine specimens were tested and two channel-die compression setups were considered: no gap between specimen/pads (specimens *biaxial loading / b*) and 0.05 mm gaps between specimen/pads (specimens *uniaxial then biaxial loading / u-b*). The biaxial tests were terminated at different load levels (Table 1). Failure was investigated using the load history, the DIC strain maps and finally using optical microscopy on post-test specimens.

Table 1. Specimen testing conditions.

Specimen	**1**	**2**	**3**	**4**	**5**	**6**	**7**	**8**	**9**
Loading type[a)]	*u*	*u*	*u-b*	*u-b*	*b*	*b*	*b*	*b*	*b*
Catastrophic failure	yes	yes	yes	no	no	no	no	no	no
σ_{33} end of test (MPa)	-207	-212	-793	-656	-815	-593	-500	-399	-300
Failure from microscopy	*n/d*	*n/d*	*n/d*	yes	*n/d*	yes	yes	no	no

[a)] *u: uniaxial loading, u-b: uniaxial then biaxial loading, b: biaxial loading*
n/d: not done

3. Results and discussion

3.1. Influence of specimen geometry for uniaxial compression

In Fig. 2, the results of the two prismatic specimens tested in compression without lateral constraint are compared to the results obtained using double waisted specimens in compression [5]. Double waisted specimens have been especially designed for the evaluation of through-thickness properties of composites [6]. The curves in Fig. 2 show that stress–strain responses are similar for both specimen types. The difference in stiffness is about 10% and the difference in failure stress about 2%.

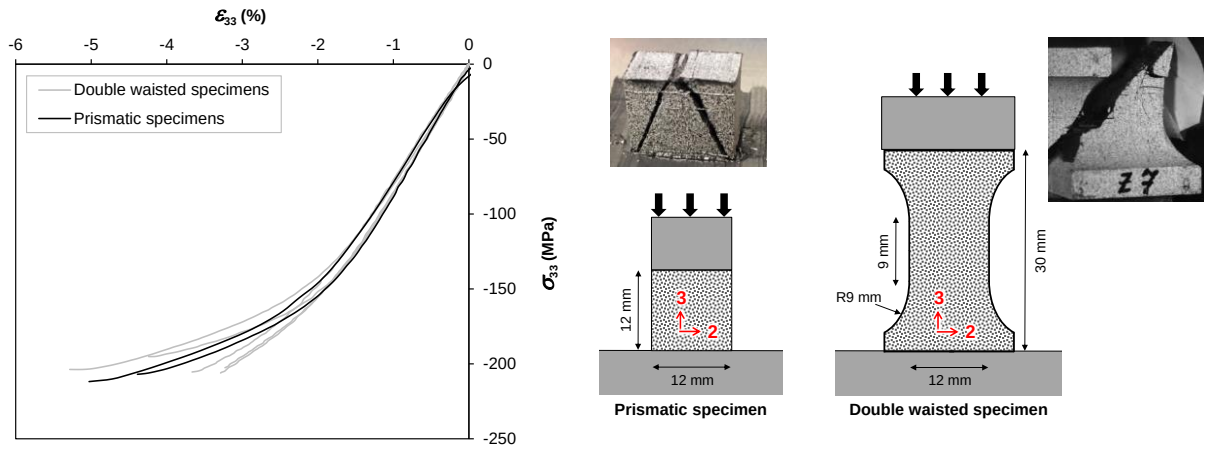

Figure 2. Compressive stress–strain response of prismatic and double waisted UD specimens.

The failure morphology was also comparable in both specimen types, i.e. the catastrophic failure during the test was characterised by one or several inclined failure planes parallel to the fibre direction. The results presented here suggest that prismatic specimens are suitable for evaluating through-thickness properties. Compared to the double waisted specimens, the prismatic specimens require thinner laminates and are easier to manufacture.

3.2. Stress response of the different specimen types

The stress response of a representative uniaxial specimen and of two biaxial specimens (with and without gaps between specimen/pads) are shown in Fig. 3. Fig. 3b) indicates that much higher compressive stresses σ_{33} are reached in biaxial transverse compression tests than in uniaxial compression tests. In fact, the specimen failure in the biaxial tests was not catastrophic and was not associated with a large load drop, as opposed to what was observed for uniaxial transverse compression. After unloading of the terminated test the biaxial specimens were still held in one piece. This is unlike the UD specimens tested under triaxial compression in [3] which fractured by shear in a neat shear failure plane. For the biaxial compression tests in [4] the level of lateral constraint was much higher than here (steel were used instead of composite pads) and the failure plane observed was going across the fibres rather than between the fibres. The stress–stress diagram in Fig. 3c) shows that the loading condition for the channel-die specimen with gaps is initially uniaxial ($\sigma_{22}\approx 0$) and then becomes biaxial. The nonlinearity in the stress–stress curves indicates a change in stress ratio and an increase of Poisson's ratio ν_{32} as result from the material degradation.

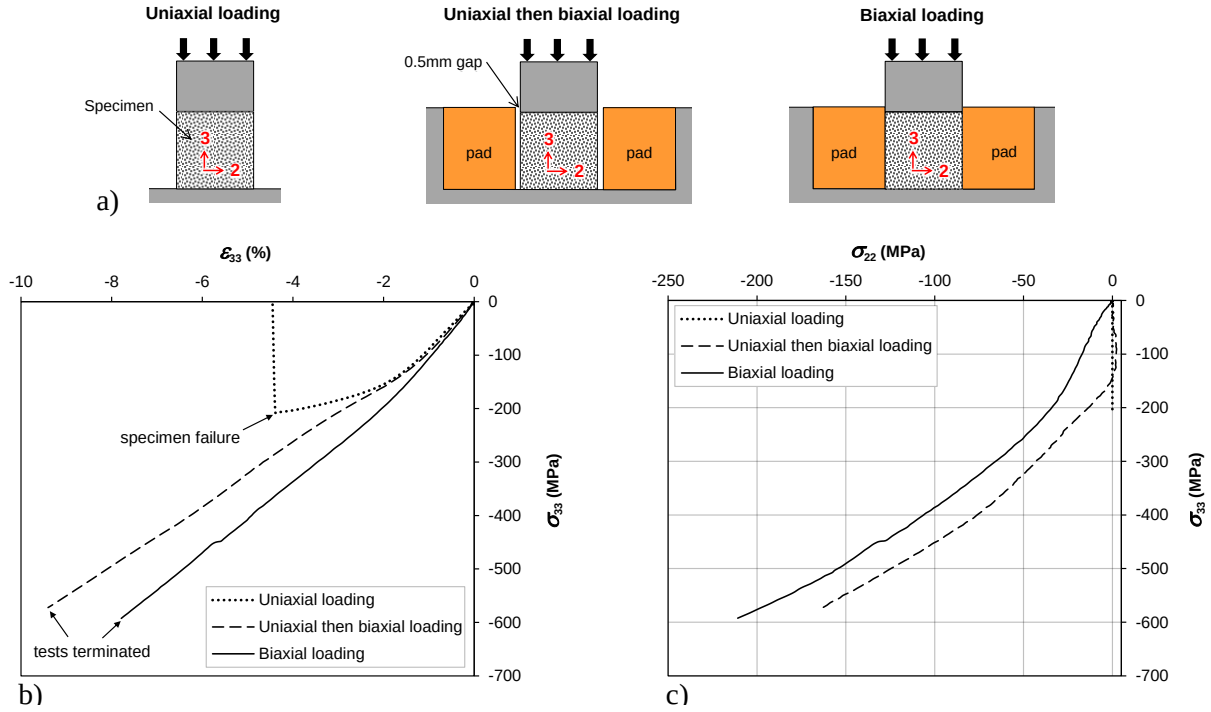

Figure 3. Uniaxial and biaxial transverse compression response for representative specimens of each type.

3.3. Definition of failure

Catastrophic failure was not observed in biaxial specimens, most likely because of the high degree of lateral constraint which prevents cracks from growing across the entire specimen. However, the post-test failure analysis revealed presence of matrix cracks through large regions of the specimens (see Fig. 4).

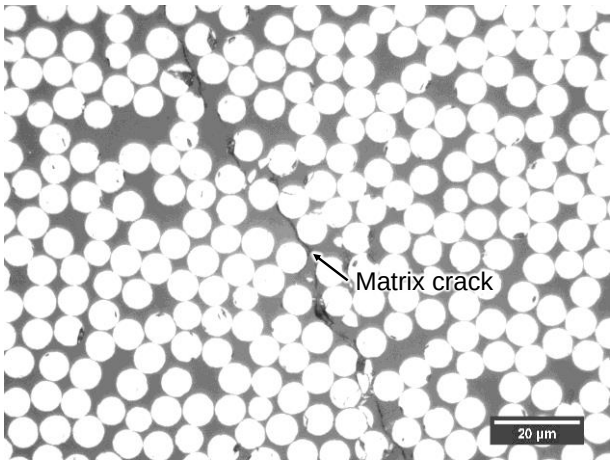

Figure 4. Matrix crack observed in an unloaded biaxial transverse compression specimen (spec. 7).

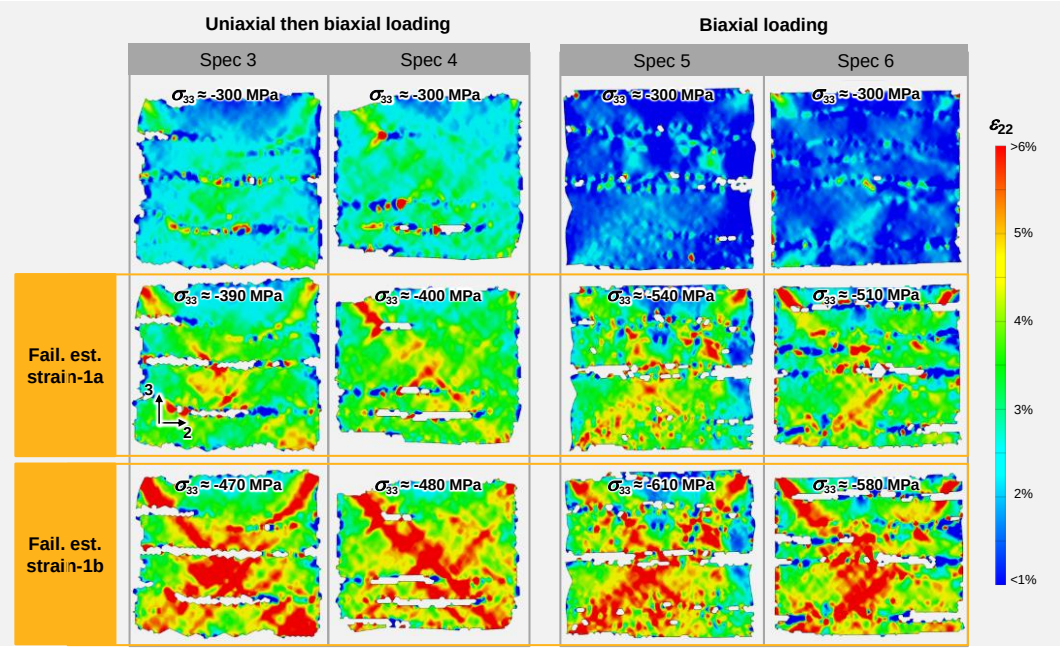

Figure 5. ε_{22} strain maps in biaxial specimens.

Also, strain localisation was observed on the DIC strain maps as a result of a matrix dominated failure. Among all strain components, the transverse strain ε_{22} was found to be the most efficient component to determine the point at which failure occurs. It is difficult to quantify exactly the stage at which strain localisation occurs because the process is relatively smooth and progressive in the strain maps. In Fig. 5 two subjective estimations of the failure stage from the interpretation of ε_{22} strain maps are

given. The first estimation (Fail. est. strain-1a) corresponds to the moment at which regions of high ε_{22} become visible at the specimen surface. The second estimation (Fail. est. strain-1b) corresponds to a higher stress level, at which the specimen strain map clearly indicates several regions of strain localisation across the specimen.

The strength determined in Fig. 5 are plotted in the σ_{22}–σ_{33} diagram in Fig. 6.The results of more objective failure evaluation methods, using the value of the standard deviation of ε_{22} (Fail. est. strain-2a/b/c), are also reported. In some cases a load disturbance could be observed during the test (e.g. in the biaxial loading curve in Fig. 3b) and the associated stress state is also reported on the failure envelope in Fig. 6. For the uniaxial specimens the stress at which catastrophic failure occurred is shown. The results indicate that independently of failure definition the strength seem to follow a linear regression in the σ_{22}–σ_{33} diagram. This linear failure envelope in compression is in accordance with the results reported in the WWFE-II, Test Case 5 [1] on the uniaxial compression of glass/epoxy 0°-laminate with superimposed hydrostatic pressure [3].

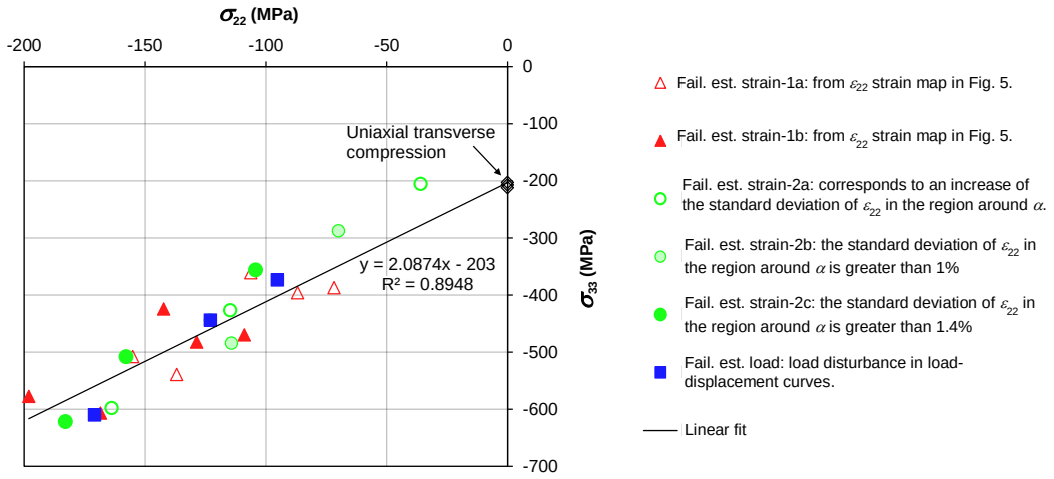

Figure 6. σ_{33}–σ_{22} failure envelope in compression.

3.4. Extraction of the shear response

The compressive stresses σ_{33} and σ_{22} can be resolved into traction components acting on the failure plane oriented with the angle α w.r.t. the thickness direction (shown in Fig. 7a) using stress transformation equations (Eq. 1 and Eq. 2). For uniaxially loaded specimens, the failure was catastrophic and a neat fracture plane could be measured on the post-mortem specimens. However, for biaxial loaded specimens no catastrophic failure was observed. Therefore, α was measured from the orientation of the regions that showed the highest ε_{22} strain. The angle α was varying between 32-49° amongst all biaxial specimens and between 39-42° for the uniaxial specimens. The ε_{22} map used to define α is shown in Fig. 7b).

$$\sigma_N = \frac{\sigma_{22}+\sigma_{33}}{2} + \frac{\sigma_{22}-\sigma_{33}}{2}\cos(2\alpha) \tag{1}$$

$$\tau_T = -\frac{\sigma_{22}-\sigma_{33}}{2}\sin(2\alpha) \tag{2}$$

In order to calculate the shear strain γ_T along the failure plane α, the coordinate system of the DIC system, originally aligned with the material coordinate system, was rotated with the angle α to the thickness direction (Fig. 7b). The local shear strain measurements were then averaged in a narrow region along the failure plane α (Fig. 7b).

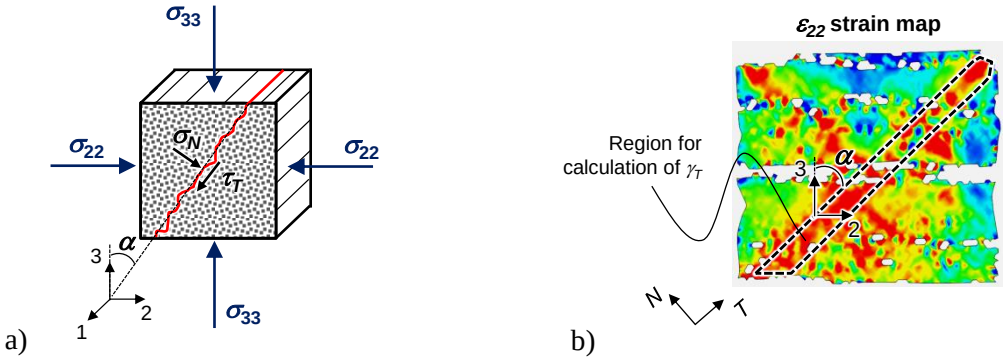

Figure 7. a) Resulting stresses acting on a failure plane during transverse biaxial loading and b) calculation of the transverse shear strain.

The resulting shear stress–strain curves τ_T–γ_T for uniaxial and biaxial transverse compression are shown in Fig. 8a). An average curve and the associated standard deviation was calculated from all the specimen tested for each loading type. Initially, the shear response is linear with a stiffness which is in good agreement with the value estimated by the transversally isotropic assumption, i.e. $G_{23}=E_T/[2(1+\nu)]=2.9$ GPa, with $E_T=(E_{22}+E_{33})/2$ and $\nu=(\nu_{23}+\nu_{32})/2$. The difference in the nonlinear behaviour of the transverse shear response between uniaxial and biaxial transverse loading conditions can be explained by the different pressure σ_N acting on the failure plane α. The experimental curves generated in Fig. 8a) are important input to material models that require transverse shear data as input. In Fig. 8b) the shear responses predicted by the matrix damage model for UD composite presented in [7] are shown. These FE results were produced for the same biaxial stress ratio as in the experiments, for the same material as in the experiments, but without any calibration of the model with the experimental biaxial results. The good agreement between the experiments and the numerical results

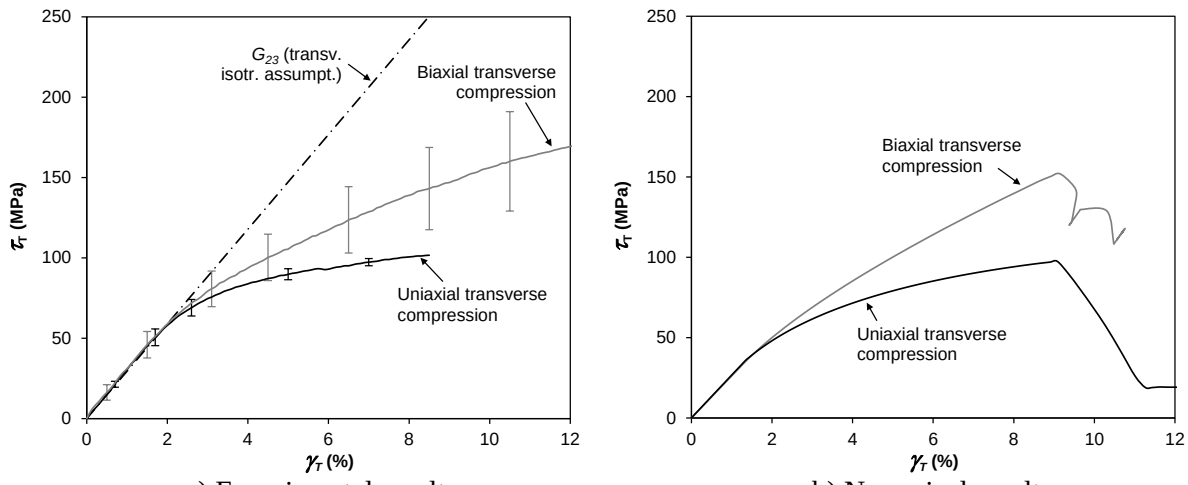

Figure 8. Transverse shear stress–strain curves a) average curve extracted from the experiments (with standard deviation bars) and b) predicted by the material model [7].

suggests that the material parameters for the transverse shear response assumed in [7] are relatively good estimations.

4. Conclusions

The behaviour of a UD carbon/epoxy laminates loaded in biaxial transverse compression was characterised. The material response exhibited some nonlinearity because of the loading being matrix dominated. Although no catastrophic specimen failure was observed the post-test failure analysis confirmed that a shear driven transverse failure had occurred. The transverse shear response of the material was extracted from the tests using stress transformation equations and rotation of DIC strain measurements along a potential failure plane.

Uniaxial transverse compression tests were also performed on prismatic and on double waisted UD specimens. It was shown that the specimen design has no noticeable influence on the stress-strain response and on the failure stress. In comparison to uniaxial compression tests, the biaxial transverse compression tests exhibited higher modulus, less degree of nonlinearity and higher strength.

Acknowledgments

The authors would like to gratefully acknowledge the funding from the Swedish Energy Agency through project 34181-2. The authors would also like to gratefully acknowledge Mr Sérgio Costa for helping identifying the experimental input needed for crash models and for assisting with simulations.

References

[1] A.S. Kaddour and M.J. Hinton. Maturity of 3D failure criteria for fibre-reinforced composites: comparison between theories and experiments: Part B of WWFE-II. *Journal of Composite Materials,* 47:925–966, 2013.

[2] A. Smits, D. Van Hemelrijck, T.P. Philippidis and A. Cardon. Design of a cruciform specimen for biaxial testing of fibre reinforced composite laminates. *Composites Science and Technology,* 66:964–975, 2006.

[3] P.J. Hine, R.A. Duckett, A.S. Kaddour, M.J. Hinton and G.M. Wells. The effect of hydrostatic pressure on the mechanical properties of glass fibre/epoxy unidirectional composites. *Composites Part A: Applied Science and Manufacturing,* 36:279–289, 2005.

[4] T.A. Collings. Transverse compressive behaviour of unidirectional carbon fibre reinforced plastics. *Composites,* 5:108–116, 1974.

[5] T. Bru, P. Hellström¸.R. Gutkin, D. Ramantani and G. Peterson. Characterisation of the mechanical and fracture properties of a uni-weave carbon fibre/epoxy non-crimp fabric composite. *Data in Brief,* 6:680–695, 2016.

[6] R.F. Ferguson, M.J. Hinton and M.J Hiley. Determining the through-thickness properties of FRP materials. *Composites Science and Technology,* 58:1411–1420, 1998.

[7] S. Costa, A. Portugal, R. Olsson, G.M. Vyas and T. Bru. Validation of a novel model for the compressive response of FRP: numerical simulation. *Proceedings of the 21st International Conference on Composite Materials ICCM-21, Xi'an, China,* August 20-25 2017.